

Invariant grids: method of complexity reduction in reaction networks

Alexander Gorban^{2,4}
ag153@leicester.ac.uk

Iliya Karlin^{1,2}
karlin@lav.mavt.ethz.ch

Andrei Zinovyev^{2,3}
andrei.zinovyev@curie.fr

¹ ETH, Swiss Federal Institute of Technology, Switzerland

² Institute of Computational Modeling SB RAS, Russia

³ Bioinformatics service of Institut Curie, France

⁴ Centre for mathematical modeling, University of Leicester

Abstract

Complexity in the description of big chemical reaction networks has both structural (number of species and reactions) and temporal (very different reaction rates) aspects. A consistent way to make model reduction is to construct the invariant manifold which describes the asymptotic system behavior. In this paper we present a discrete analog of this object: an invariant grid. Invariant grid is introduced independently from the invariant manifold notion and can serve itself to represent the dynamic system behavior as well as to approximate the invariant manifold after refinement. The method is designed for pure dissipative systems and widely uses their thermodynamic properties but allows also generalizations for some classes of open systems. The method is illustrated by two examples: the simplest catalytic reaction (Michaelis-Menten mechanism) and the hydrogen oxidation.

Keywords: Kinetics; Model Reduction; Grids; Invariant Manifold; Entropy; Nonlinear Dynamics; Mathematical Modeling; Numerical methods

Running title: Method of invariant grid

Corresponding author: Andrei Zinovyev, Institut Curie, Service Bioinformatique, rue d'Ulm, 26, 75248, Paris, France. Tel: +33 1 42 34 65 27; Fax: +33 1 42 34 65 28.

1 Introduction

Reaction networks serve as a good model to imitate and predict behavior of complex systems of interacting components. Modern research faces with constantly increasing complexity of the systems under study: as a good example, nowadays one can observe a boom connected with studies of biochemical processes in a living cell (for recent overviews, see [1],[2]). There is no need to underline emerging needs for the methods of reducing the complexity of system description and behavior.

Complexity in modeling big chemical reaction networks has both structural (number of species and reactions) and temporal (very different reaction rates) aspects, see Fig. 1. In general, it is not possible to disregard the temporal organization of the network when one wants to create a realistic system model. Of course, the rate constants and reaction laws are rarely available completely. This makes extremely desirable the development of methods allowing to reduce the number of system parameters as well as methods for qualitative analysis of chemical reaction networks [2].

The idea of model reduction with respect to slow motion extraction can be introduced as follows: we have a system of ordinary differential equations describing time evolution of n species concentrations (or masses) in time:

$$\frac{d\mathbf{x}}{dt} = J(\mathbf{x}), \quad (1)$$

Every particular state of the system corresponds to a point in the phase space U and the system dynamics is determined by the vector field $J(x)$, $x \in U$. We construct new (reduced) dynamics

$$\frac{d\mathbf{y}}{dt} = J'(\mathbf{y}), \quad (2)$$

where $y_i, i = 1..m, m \ll n$ is a new set of variables corresponding to slow dynamics of the initial system (1). By analogy with statistical physics it corresponds to the "macroscopic" description of the chemical system (we observe only effects of slow system changes, comparable in time scale with characteristic times of experimental measurements) as opposite to "microscopic" variables x_i . The reduced system dynamics exists on a m -dimensional manifold (surface) Ω embedded in the n -dimensional phase space and defined by functions $x_i = x_i(y_1, \dots, y_m)$.

A consistent way for model reduction is to construct a positively invariant slow manifold Ω_{inv} , such that if an individual trajectory of the system (1) has started on Ω_{inv} , it does not leave Ω_{inv} anymore, i.e. the vector field $J(x)$ in the points of the manifold is tangent to it, Fig. 2a. The 'ideal' picture of the reduced description we have in mind is as follows: A typical phase trajectory, $x(t)$, where t is the time, and x is an element of the phase space, consists of two pronounced segments. The first segment connects the beginning of the trajectory, $x(0)$, with a certain point, $x(t_1)$, on the manifold Ω_{inv} (rigorously speaking, we should think of $x(t_1)$ not on Ω_{inv} but in a small neighborhood of Ω_{inv} but this is inessential for the ideal picture). The second segment belongs to Ω_{inv} . Thus, the manifolds appearing in our ideal picture are "patterns" formed by the segments of individual trajectories, and the goal of the reduced description is to "filter out" this manifold (Fig. 2a).

Usually construction of invariant manifold in the explicit form is difficult. Most of the time one deals with its approximation constructed using some method (see, for overview, [6], [8], [4], [5]). It is formally possible to induce new dynamics on any given manifold Ω , not necessarily invariant, if one introduces a projector operator P of the vector field on the tangent bundle of the manifold Ω : $PJ(x \in \Omega) \in T_x\Omega$. By definition, the manifold Ω is invariant with respect to the vector field J if and only if the following equality is true for each $x \in \Omega$:

$$[1 - P]J(x) = 0, \quad (3)$$

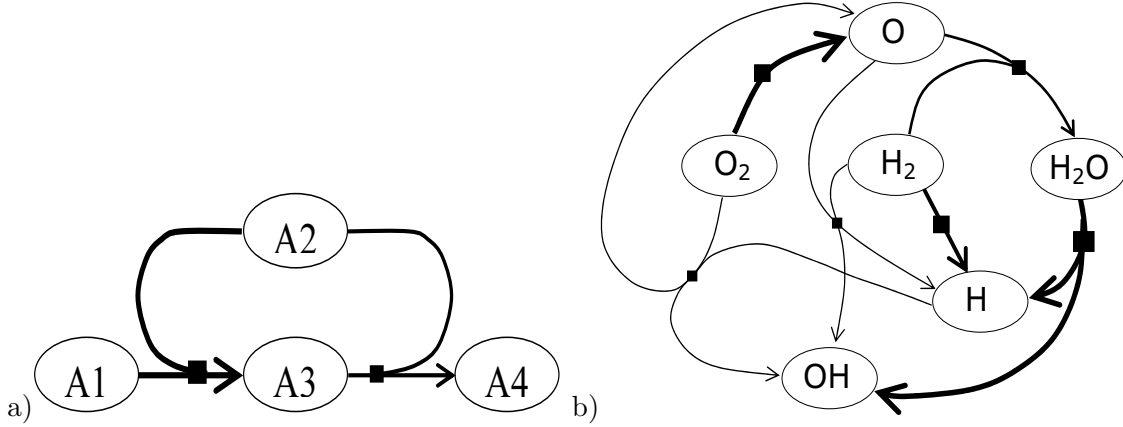


Figure 1: Graphical representation of two model systems considered as examples in this paper: a) Michaelis-Menten mechanism; b) Hydrogen burning model with 6 variables. Here circles represent chemical species, squares represent chemical reactions. Line widths reflect direct reaction rate constants, thicker line corresponds to a slower reaction (in a logarithmic scale). All reactions here are governed by mass action law and supposed to be reversible.

where projector P depends on the point x and on the manifold Ω in the vicinity of x . This equation is a differential equation for functions that define the manifold Ω . Newton method and relaxation method, both iterative, were proposed to find a sequence of corrections to some initial approximation Ω , in such a way that every next approximation has less *invariance* defect $[1 - P]J(x)$, see [5]. These corrections can be performed analytically in some cases.

For the case of a complex chemical reaction network, one has to develop a computationally effective method of invariant manifold construction. If one constructs a surface of a relatively low dimension, grid-based manifold representations become a relevant option [8]. In this paper we present such an approach named *method of invariant grids* (MIG). From one hand, grid representation can be refined and converge more and more closely to the invariant manifold. From the other, we define *invariant grid* as an object independent on the manifold itself. Thus, it can be used independently: for example, for visualization of the global system dynamics as it will be shown in the end of this paper.

Invariant grid is an undirected graph which consists of a set of nodes and connections between them. The graph can be represented in two spaces: in the low-dimensional space of the internal (reduced) coordinates where it forms a finite lattice (usually, regular and rectangular or hexagonal), and, simultaneously, it is embedded in the phase space U , thus every node corresponds to a species concentrations vector \mathbf{x} . Using connectivity of the graph, one can introduce differentiation operators and calculate the tangent vectors and define the projector operator in every node. This is the only place where the connectivity of the graph is used. The node positions in U are optimized such that the invariance condition (3) is satisfied *for every node*. In this paper we propose two algorithms for how to do it, both iterative: of Newton type and a relaxation method. After node positions optimization the grid is called *invariant*.

In this study we consider class of dissipative systems, i.e. such systems for which there exists a global convex Lyapunov function G (thermodynamic potential) which implements the second law of thermodynamics. For example, because of this reason, all reactions on Fig. 1 are reversible. Dissipative systems have the only steady state in the equilibrium point and as the time t tends to infinity, the system reaches the equilibrium state while in the course of the transition the Lyapunov function decreases monotonically. Thermodynamic properties of dissipative systems help a lot: for example, they unambiguously define metrics in the phase space to perform geometrical calculations and also define the choice of projector P almost uniquely (see the next section).

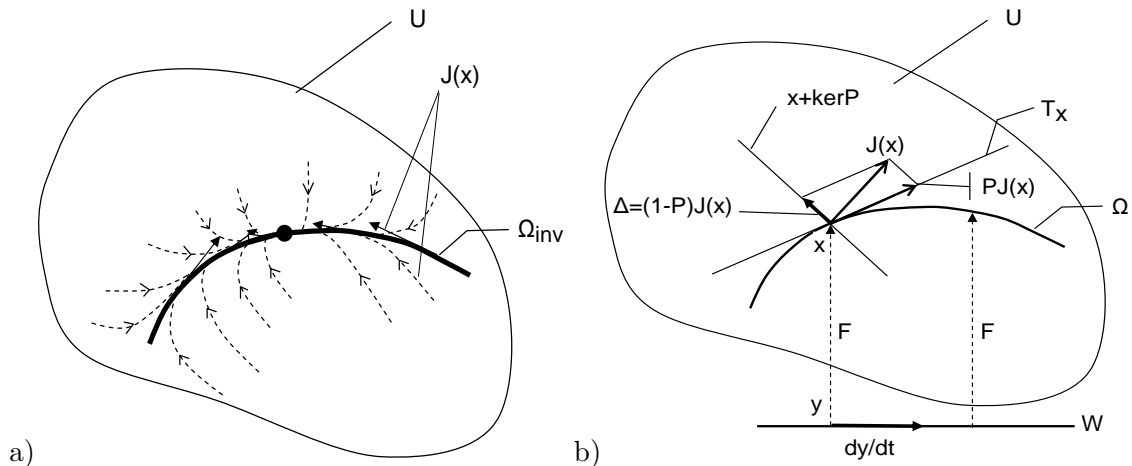


Figure 2: Main geometrical structures of model reduction: U is the phase space, $J(x)$ is the vector field of the system under consideration: $dx/dt = J(x)$, Ω is an ansatz manifold, W is the space of macroscopic variables (coordinates on the manifold), the map $F : W \rightarrow U$ maps any point $y \in W$ into the corresponding point $x = F(y)$ on the manifold Ω , T_x is the tangent space to the manifold Ω at the point x , $PJ(x)$ is the projection of the vector $J(x)$ onto tangent space T_x , the vector field dy/dt describes the induced dynamics on the space of parameters, $\Delta = (1 - P)J(x)$ is the defect of invariance, the affine subspace $x + \ker P$ is the plane of fast motions, and $\Delta \in \ker P$. a) Here Ω_{inv} is an invariant manifold (all $J(x \in \Omega_{inv})$ are tangent to Ω_{inv}) and a possible dynamics is shown in its vicinity; b) here Ω is some manifold approximating the invariant manifold ($J(x \in \Omega)$ is not necessarily tangent to Ω), one can use operator P to derive new dynamics (2).

Low dimensional invariant manifolds exist also for systems with a more complicated dynamic behavior so why to study the invariant manifolds of slow motions for a particular class of purely dissipative systems? The answer is in the following: Most of the physically significant models include non-dissipative components in a form of either a conservative dynamics or in the form of external fluxes. For example, one can think of irreversible reactions among the suggested stoichiometric mechanism (inverse process are so improbable that we discard them completely thereby effectively “opening” the system to the remaining irreversible flux). For all such systems, the method of invariant grids is applicable almost without special refinements, and bears the significance that invariant manifolds are constructed as a “deformation” of the relevant manifolds of slow motion of the purely dissipative dynamics. Example of this construction for open systems is presented below in the last section of the paper. The calculations in the last chapter do not use grid specifics and can be applied not only for grid representation of the invariant manifold, but also for any analytical form of its representation.

2 Dissipative systems and thermodynamic projector

2.1 Kinetic equations

Let us introduce the notions used in the paper (see also [3], [9], [7]). We will consider a closed system with n chemical species A_1, \dots, A_n , participating in a complex reaction. The complex reaction is represented by the following stoichiometric mechanism:



where the index $s = 1, \dots, r$ enumerates the reaction steps, and where integers, α_{si} and β_{si} , are stoichiometric coefficients. For each reaction step s , we introduce n -component vectors α_s and β_s with components α_{si} and β_{si} . Notation γ_s stands for the vector with integer components $\gamma_{si} = \beta_{si} - \alpha_{si}$ (the stoichiometric vector).

For every A_i an *extensive variable* N_i , “the number of particles of that species”, is defined. The concentration of A_i is $x_i = N_i/V$, where V is the volume.

Given the stoichiometric mechanism (4), the reaction kinetic equations read:

$$\dot{\mathbf{N}} = V\mathbf{J}(\mathbf{x}), \quad \mathbf{J}(\mathbf{x}) = \sum_{s=1}^r \gamma_s W_s(\mathbf{x}), \quad (5)$$

where dot denotes the time derivative, and W_s is the reaction rate function of the step s . In particular, *the mass action law* suggests the polynomial form of the reaction rates:

$$W_s(\mathbf{x}) = W_s^+(\mathbf{x}) - W_s^-(\mathbf{x}) = k_s^+(T) \prod_{i=1}^n x_i^{\alpha_i} - k_s^-(T) \prod_{i=1}^n x_i^{\beta_i}, \quad (6)$$

where $k_s^+(T)$ and $k_s^-(T)$ are the constants of the direct and of the inverse reactions rates of the s th reaction step, T is the temperature.

The rate constants are not independent. The *principle of detail balance* gives the following connection between these constants: There exists such a positive vector $\mathbf{x}^{\text{eq}}(T)$ that

$$W_s^+(\mathbf{x}^{\text{eq}}) = W_s^-(\mathbf{x}^{\text{eq}}) \text{ for all } s = 1, \dots, r. \quad (7)$$

For $V, T = \text{const}$ we do not need additional equations and data. It is possible simply to divide equation (5) by the constant volume and to write

$$\dot{\mathbf{x}} = \sum_{s=1}^r \gamma_s W_s(\mathbf{x}). \quad (8)$$

Conservation laws (balances) impose linear constraints on admissible vectors \mathbf{x} :

$$(\mathbf{b}_i, \mathbf{x}) = B_i = \text{const}, \quad i = 1, \dots, l, \quad (9)$$

where \mathbf{b}_i are fixed and linearly independent vectors. Let us denote as \mathbf{B} the set of vectors which satisfy the conservation laws (9) with given B_i :

$$\mathbf{B} = \{\mathbf{x} | (\mathbf{b}_1, \mathbf{x}) = B_1, \dots, (\mathbf{b}_l, \mathbf{x}) = B_l\}.$$

The natural phase space \mathbf{X} of the system (8) is the intersection of the cone of n -dimensional vectors with nonnegative components, with the set \mathbf{B} , and $\dim \mathbf{X} = d = n - l$. In addition, we assume that each of the conservation laws is supported by each elementary reaction step, that is

$$(\gamma_s, \mathbf{b}_i) = 0, \quad (10)$$

for each pair of vectors γ_s and \mathbf{b}_i .

We assume that the kinetic equation (8) describes evolution towards the unique equilibrium state, \mathbf{x}^{eq} , in the interior of the phase space \mathbf{X} . Furthermore, we assume that there exists a strictly convex function $G(\mathbf{x})$ which decreases monotonically in time due to (8):

$$\dot{G} = (\nabla G(\mathbf{x}), \mathbf{J}(\mathbf{x})) \leq 0. \quad (11)$$

Here ∇G is the vector of partial derivatives $\partial G / \partial x_i$, and the convexity assumes that the $n \times n$ matrices

$$\mathbf{H}_{\mathbf{x}} = \|\partial^2 G(\mathbf{x}) / \partial x_i \partial x_j\|, \quad (12)$$

are positive definite for all $\mathbf{x} \in \mathbf{X}$. In addition, we assume that the matrices (12) are invertible if \mathbf{x} is taken in the interior of the phase space.

The matrix \mathbf{H} defines an important Riemann structure on the concentration space, the thermodynamic (or entropic) scalar product:

$$\langle \mathbf{x}, \mathbf{y} \rangle_c = (\mathbf{x}, \mathbf{H}_x \mathbf{y}), \quad (13)$$

This choice of the Riemann structure is unambiguous from the thermodynamic perspective. We use this metrics for all geometrical constructions, for measuring angles and distances in the phase space U .

The function G is the Lyapunov function of the system (5), and \mathbf{x}^{eq} is the point of global minimum of the function G in the phase space \mathbf{X} . Otherwise stated, the manifold of equilibrium states $\mathbf{x}^{\text{eq}}(B_1, \dots, B_l)$ is the solution to the variational problem,

$$G \rightarrow \min \text{ for } (b_i, \mathbf{x}) = B_i, \quad i = 1, \dots, l. \quad (14)$$

For each fixed value of the conserved quantities B_i , the solution is unique.

For perfect systems in a constant volume under a constant temperature, the Lyapunov function G reads:

$$G = \sum_{i=1}^n x_i [\ln(x_i/x_i^{\text{eq}}) - 1]. \quad (15)$$

2.2 Thermodynamic projector

For dissipative systems, we keep in mind the following picture (Fig. 2). The vector field $J(x)$ generates the motion on the phase space U : $dx/dt = J(x)$. An ansatz manifold Ω is given, it is the current approximation to the invariant manifold. This manifold Ω is described as the image of the map $F : W \rightarrow U$, where W is a space of macroscopic variables, U is our phase space.

The projected vector field $PJ(x)$ belongs to the tangent space T_x , and the equation $dx/dt = PJ(x)$ describes the motion along the ansatz manifold Ω (if the initial state belongs to Ω). The induced dynamics on the space W is generated by the vector field

$$\frac{dy}{dt} = (D_y F)^{-1} PJ(F(y)).$$

Here the inverse linear operator $(D_y F)^{-1}$ is defined on the tangent space $T_{F(y)}$, because the map F is assumed to be immersion, that is the differential $(D_y F)$ is the isomorphism onto the tangent space $T_{F(y)}$.

Projection operators P contribute to the invariance equation (3). Limiting results, exact solutions, etc. only weakly depend on the particular choice of projectors, or do not depend on it at all. However, thermodynamical validity of approximations obtained on each iteration step towards the limit strongly depends on the choice of the projector.

Let *some* (not obligatory invariant) manifold Ω is considered as a manifold of reduced description. We should define a field of linear operators, \mathbf{P}_x , labeled by the states $\mathbf{x} \in \Omega$, which project the vectors $\mathbf{J}(\mathbf{x})$, $\mathbf{x} \in \Omega$ onto the tangent bundle of the manifold Ω , thereby generating the induced vector field, $\mathbf{P}_x \mathbf{J}(\mathbf{x})$, $\mathbf{x} \in \Omega$. This induced vector field on the tangent bundle of the manifold Ω is identified with the reduced dynamics along the manifold Ω . The *thermodynamicity* requirement for this induced vector field reads

$$(\nabla G(\mathbf{x}), \mathbf{P}_x \mathbf{J}(\mathbf{x})) \leq 0, \text{ for each } \mathbf{x} \in \Omega. \quad (16)$$

The condition (16) means that the entropy (which is the Lyapunov function with minus sign) should increase in the new dynamics (2).

How to construct the projector P ? Another form of this question is: how to define the plain of fast motions $x + \ker P$? The choice of the projector P is ambiguous, from the formal point

of view, but the second law of thermodynamics gives a good hint [3]: the entropy should grow in the fast motion, and the point x should be the point of entropy maximum on the plane of fast motion $x + \ker P$. That is, the subspace $\ker P$ should belong to the kernel of the entropy differential:

$$\ker P_x \subset \ker D_x S.$$

Of course, this rule is valid for closed systems with entropy, but it can be also extended onto open systems: the projection of the “thermodynamic part” of $J(x)$ onto T_x should have the positive entropy production. If this thermodynamic requirement is valid for any ansatz manifold not tangent to the entropy levels and for any thermodynamic vector field, then the thermodynamic projector is unique [13]. Let us describe this projector P for a given point x , subspace $T_x = \text{im} P$, differential $D_x S$ of the entropy S at the point x and the second differential of the entropy at the point x , the bilinear functional $(D_x^2 S)_x$. We need the positively definite bilinear form $\langle z|p \rangle_x = -(D_x^2 S)_x(z, p)$ (the entropic scalar product). There exists a unique vector g such that $\langle g|p \rangle_x = D_x S(p)$. It is the Riesz representation of the linear functional $D_x S$ with respect to entropic scalar product. If $g \neq 0$ then the thermodynamic projector is

$$P(J) = P^\perp(J) + \frac{g^\parallel}{\langle g^\parallel|g^\parallel \rangle_x} \langle g^\perp|J \rangle_x, \quad (17)$$

where P^\perp is the orthogonal projector onto T_x with respect to the entropic scalar product, and the vector g is splitted onto tangent and orthogonal components:

$$g = g^\parallel + g^\perp; \quad g^\parallel = P^\perp g; \quad g^\perp = (1 - P^\perp)g.$$

This projector is defined if $g^\parallel \neq 0$.

If $g = 0$ (the equilibrium point) then $P(J) = P^\perp(J)$.

For given T_x , the *thermodynamic projector* (17) depends on the point x through the x -dependence of the scalar product $\langle | \rangle_x$, and also through the differential of S in x .

2.3 Symmetric linearization

The invariance condition (3) supports a lot of invariant manifolds, and not all of them are relevant to the reduced description (for example, any individual trajectory is itself an invariant manifold). This should be carefully taken into account when deriving a relevant equation for the correction in the states of the initial manifold Ω_0 which are located far from equilibrium. This point concerns the procedure of the linearization of the vector field \mathbf{J} , appearing in the equation (1). Let \mathbf{c} is an arbitrary point of the phase space. The linearization of the vector function \mathbf{J} about \mathbf{c} may be written $J(\mathbf{c} + \delta\mathbf{c}) \approx \mathbf{J}(\mathbf{c}) + \mathbf{L}_\mathbf{c}\delta\mathbf{c}$ where the linear operator $\mathbf{L}_\mathbf{c}$ acts as follows (for the mass action law):

$$\mathbf{L}_\mathbf{c}\mathbf{x} = \sum_{s=1}^r \gamma_s [W_s^+(\mathbf{c})(\alpha_s, \mathbf{H}_\mathbf{c}\mathbf{x}) - W_s^-(\mathbf{c})(\beta_s, \mathbf{H}_\mathbf{c}\mathbf{x})]. \quad (18)$$

Here $\mathbf{H}_\mathbf{c}$ is the matrix of second derivatives of the function G in the state \mathbf{c} , see (12). The matrix $\mathbf{L}_\mathbf{c}$ in (18) can be decomposed as follows:

$$\mathbf{L}_\mathbf{c} = \mathbf{L}'_\mathbf{c} + \mathbf{L}''_\mathbf{c}. \quad (19)$$

Matrices $\mathbf{L}'_\mathbf{c}$ and $\mathbf{L}''_\mathbf{c}$ act as follows:

$$\mathbf{L}'_\mathbf{c}\mathbf{x} = -\frac{1}{2} \sum_{s=1}^r [W_s^+(\mathbf{c}) + W_s^-(\mathbf{c})] \gamma_s (\gamma_s, \mathbf{H}_\mathbf{c}\mathbf{x}), \quad (20)$$

$$\mathbf{L}''_\mathbf{c}\mathbf{x} = \frac{1}{2} \sum_{s=1}^r [W_s^+(\mathbf{c}) - W_s^-(\mathbf{c})] \gamma_s (\alpha_s + \beta_s, \mathbf{H}_\mathbf{c}\mathbf{x}). \quad (21)$$

Some features of this decomposition are best seen when we use the thermodynamic scalar product (13): The following properties of the matrix $\mathbf{L}'_{\mathbf{c}}$ are verified immediately:

(i) The matrix $\mathbf{L}'_{\mathbf{c}}$ is symmetric in the scalar product (13):

$$\langle \mathbf{x}, \mathbf{L}'_{\mathbf{c}} \mathbf{y} \rangle = \langle \mathbf{y}, \mathbf{L}'_{\mathbf{c}} \mathbf{x} \rangle. \quad (22)$$

(ii) The matrix $\mathbf{L}'_{\mathbf{c}}$ is nonpositive definite in the scalar product (13):

$$\langle \mathbf{x}, \mathbf{L}'_{\mathbf{c}} \mathbf{x} \rangle \leq 0. \quad (23)$$

(iii) The null space of the matrix $\mathbf{L}'_{\mathbf{c}}$ is the linear envelope of the vectors $\mathbf{H}_{\mathbf{c}}^{-1} \mathbf{b}_i$ representing the complete system of conservation laws:

$$\ker \mathbf{L}'_{\mathbf{c}} = \text{Lin}\{\mathbf{H}_{\mathbf{c}}^{-1} \mathbf{b}_i, i = 1, \dots, l\} \quad (24)$$

(iv) If $\mathbf{c} = \mathbf{c}^{\text{eq}}$, then $W_s^+(\mathbf{c}^{\text{eq}}) = W_s^-(\mathbf{c}^{\text{eq}})$, and

$$\mathbf{L}'_{\mathbf{c}^{\text{eq}}} = \mathbf{L}_{\mathbf{c}^{\text{eq}}}. \quad (25)$$

Thus, the decomposition (19) splits the matrix $\mathbf{L}_{\mathbf{c}}$ in two parts: one part, (20) is symmetric and nonpositive definite, while the other part, (21), vanishes in the equilibrium. The decomposition (19) explicitly takes into account the mass-action law. For other dissipative systems, the decomposition (19) is possible as soon as the relevant kinetic operator is written in a gain-loss form.

3 Invariant grids

In most of the works (of us and of other people on similar problems), analytic forms were required to represent manifolds (see, however, the method of Legendre integrators [14, 15, 16]). However, in order to construct manifolds of a relatively low dimension, grid-based representations of manifolds become a relevant option [8].

The main idea of the method of invariant grids (MIG) is to find a mapping of the finite-dimensional grids into the phase space of a dynamic system. That is, we construct not just a point approximation of the invariant manifold $F^*(y)$, but an *invariant grid*. When refined, it is expected to converge, of course, to $F^*(y)$, but in any case it is a separate, independently defined object.

Let's denote $L = R^n$, G is a discrete subset of R^n . It is natural to think of a regular grid, but this is not so crucial. For every point $y \in G$, a neighborhood of y is defined: $V_y \subset G$, where V_y is a finite set, and, in particular, $y \in V_y$. On regular grids, V_y includes, as a rule, the nearest neighbors of y . It may also include the points next to the nearest neighbors.

For our purpose, we should define a grid differential operator. For every function, defined on the grid, also all derivatives are defined:

$$\left. \frac{\partial f}{\partial y_i} \right|_{y \in G} = \sum_{z \in V_y} q_i(z, y) f(z), i = 1, \dots, n. \quad (26)$$

where $q_i(z, y)$ are some coefficients.

Here we do not specify the choice of the functions $q_i(z, y)$. We just mention in passing that, as a rule, equation (26) is established using some approximation of f in the neighborhood of y in R^n by some differentiable functions (for example, polynomials). This approximation is based on the values of f at the points of V_y . For regular grids, $q_i(z, y)$ are functions of the difference $z - y$. For some of the nodes y which are close to the edges of the grid, functions are defined only

on the part of V_y . In this case, the coefficients in (26) should be modified appropriately in order to provide an approximation using available values of f . Below we assume this modification is always done. We also assume that the number of points in the neighborhood V_y is always sufficient to make the approximation possible. This assumption restricts the choice of the grids G . Let's call *admissible* all such subsets G , on which one can define differentiation operator in every point.

Let F be a given mapping of some admissible subset $G \subset R^n$ into U . For every $y \in V$ we define tangent vectors:

$$T_y = \text{Lin}\{g_i\}_1^n, \quad (27)$$

where vectors $g_i (i = 1, \dots, n)$ are partial derivatives (26) of the vector-function F :

$$g_i = \frac{\partial F}{\partial y_i} = \sum_{z \in V_y} q_i(z, y) F(z), \quad (28)$$

or in the coordinate form:

$$(g_i)_j = \frac{\partial F_j}{\partial y_i} = \sum_{z \in V_y} q_i(z, y) F_j(z). \quad (29)$$

Here $(g_i)_j$ is the j th coordinate of the vector (g_i) , and $F_j(z)$ is the j th coordinate of the point $F(z)$.

The grid G is *invariant*, if for every node $y \in G$ the vector field $J(F(y))$ belongs to the tangent space T_y (here J is the right hand side of the kinetic equations (1)).

So, the definition of the invariant grid includes:

1. The finite admissible subset $G \subset R^n$;
2. A mapping F of this admissible subset G into U (where U is the phase space of kinetic equation (1));
3. The differentiation formulas (26) with given coefficients $q_i(z, y)$;

The *grid invariance equation* has a form of an inclusion:

$$J(F(y)) \in T_y \text{ for every } y \in G,$$

or a form of an equation:

$$(1 - P_y)J(F(y)) = 0 \text{ for every } y \in G,$$

where P_y is the thermodynamic projector (17).

The grid differentiation formulas (26) are needed, in the first place, to establish the tangent space T_y , and the null space of the thermodynamic projector P_y in each node. It is important to realize that the locality of the construction of the thermodynamic projector enables this without a global parametrization.

Let $x = F(y)$ be the location of the grid's node y immersed into U . We have the set of tangent vectors $g_i(x)$, defined in x (28), (29). Thus, the tangent space T_y is defined by (27). Also, one has the entropy function $S(x)$, the linear functional $D_x S|_x$, and the subspace $T_{0y} = T_y \cap \ker D_x S|_x$ in T_y . Let $T_{0y} \neq T_y$. In this case we have a vector $e_y \in T_y$, orthogonal to T_{0y} , $D_x S|_x(e_y) = 1$. Then the thermodynamic projector is defined as:

$$P_y \bullet = P_{0y} \bullet + e_y D_x S|_x \bullet, \quad (30)$$

where P_{0y} is the orthogonal projector on T_{0y} with respect to the entropic scalar product $\langle | \rangle_x$.

If $T_{0y} = T_y$, then the thermodynamic projector is the orthogonal projector on T_y with respect to the entropic scalar product $\langle | \rangle_x$.

The general schema of solving the invariance equation (3) to optimize positions of the invariant grid nodes in space is the following:

0) The grid is initialized. For example, one can use spectral decomposition of $(D_x^2 S)_x$ in the equilibrium;

1) Given some node positions, one calculates the tangent vectors in every node of the grid (27), at this stage the connectivity between nodes is used;

2) With set of tangent vectors calculated at the previous step, solve the invariance equation for every node *independently* and calculate a shift δy of every node in the phase space; we propose two algorithms to calculate the shift: *the Newton method with incomplete linearization* and *the relaxation method* (see also [6],[8], [5], [4]).

3) Repeat steps 1) and 2) until some convergence criterion will be fulfilled: for example, all shifts $\delta y_i, i = 1..n$ will be less than a predefined ϵ_{conv} .

4) Update the structure of the grid: for example, add new nodes and extend (extrapolate) or refine (interpolate) the grid. Some strategies for this are described further;

5) Repeat steps 1)-4) until some criterion will be fulfilled: typically, when the nodes reach the phase space boundary or the spectral gap is too small (see further).

The idea of the Newton method with incomplete linearization is to use linear approximation of J in the vicinity of a grid node y (keeping the projector P fixed). At the same time the node is shifted in the fast direction (in $y + \ker P_y$ affine subspace).

For the Newton method with incomplete linearization, the equations for calculation the new node location $y' = y + \delta y$ are:

$$\begin{cases} P_y \delta y = 0 \\ (1 - P_y)(J(y) + DJ(y)\delta y) = 0. \end{cases} \quad (31)$$

Here $DJ(y)$ is a matrix of derivatives of J evaluated at y . Instead of $DJ(y)$ (especially in the regions that are far from the equilibrium) one can use the symmetric operator $L'(y)$ (20), this will provide better convergence towards the "true" invariant manifold.

Equation (31) is a system of linear algebraic equations. In practice, it proves convenient to choose some orthonormal (with respect to the entropic scalar product) basis \mathbf{b}_i in $\ker P_y$. Let $r = \dim(\ker P_y)$. Then $\delta y = \sum_{i=1}^r \delta_i \mathbf{b}_i$, and system (31) takes the form

$$\sum_{k=1}^r \delta_k \langle \mathbf{b}_i | DJ(y) \mathbf{b}_k \rangle_y = -\langle J(y) | \mathbf{b}_i \rangle_y, i = 1...r. \quad (32)$$

This is the system of linear equations for adjusting the node location according to the Newton method with incomplete linearization. We remind once again that one should use the entropic scalar products.

For the relaxation method, one needs to calculate the defect $\Delta_y = (1 - P_y)J(y)$, and the relaxation step

$$\tau(y) = -\frac{\langle \Delta_y | \Delta_y \rangle_y}{\langle \Delta_y | DJ(y) \Delta_y \rangle_y}. \quad (33)$$

Then, the new node location y' is computed as

$$y' = y + \tau(y) \Delta_y. \quad (34)$$

This is the equation for adjusting the node location according to the relaxation method.

4 Grid construction strategy

From all the reasonable strategies of the invariant grid construction we consider here the following two: the *growing lump* and the *invariant flag*.

4.1 Growing lump

The construction is initialized from the equilibrium point y^* . The first approximation is constructed as $F(y^*) = x^*$, and for some initial V_0 ($V_{y^*} \subset V_0$) one has $F(y) = x^* + A(y - y^*)$, where A is an isometric embedding (in the standard Euclidean metrics) of R^n in E .

For this initial grid one makes a fixed number of iterations of one of the methods chosen (Newton's method with incomplete linearization or the relaxation method), and, after that, puts $V_1 = \bigcup_{y \in V_0} V_y$ and extends F from V_0 onto V_1 using the linear extrapolation, and the process continues. One of the possible variants of this procedure is to extend the grid from V_i to V_{i+1} not after a fixed number of iterations, but only after the invariance defect Δ_y becomes less than a given ϵ (in a given norm, which is entropic, as a rule), for all nodes $y \in V_i$. The lump stops growing after it reaches the boundary and is within a given accuracy $\|\Delta\| < \epsilon$.

4.2 Invariant flag

In order to construct the invariant flag one uses sufficiently regular grids G , in which many points are located on the coordinate lines, planes, etc. One considers the standard flag $R^0 \subset R^1 \subset R^2 \subset \dots \subset R^n$ (every next space is constructed by adding one more coordinate). It corresponds to a sequence of grids $\{y^*\} \subset G^1 \subset G^2 \dots \subset G^n$, where $\{y^*\} = R^0$, and G^i is a grid in R^i .

First, y^* is mapped on x^* and further $F(y^*) = x^*$. Then the invariant grid is constructed on $V^1 \subset G^1$ (up to the boundaries and within a given accuracy $\|\Delta\| < \epsilon$). After that, the neighborhoods in G^2 are added to the points V^1 , and the grid $V^2 \subset G^2$ is constructed (up to the boundaries and within a given accuracy) and so on, until $V^n \subset G^n$ is constructed.

While constructing the k th-order grid $V^k \subset G^k$, the important role of the grids of lower dimension $V^0 \subset \dots \subset V^{k-1} \subset V^k$ embedded in it, is preserved. The point $F(y^*) = x^*$ (equilibrium) remains fixed. For every $y \in V^q$ ($q < k$) the tangent vectors g_1, \dots, g_q are constructed, using the differentiation operators (26) on the whole V^k . Using the tangent space $T_y = \text{Lin}\{g_1, \dots, g_q\}$, the projector P_y is constructed, the iterations are applied and so on. All this is done in order to obtain a sequence of embedded invariant grids, given by the same map F .

4.3 Boundaries check and the entropy

We construct grid mapping of F onto a finite set $V \in G$. The technique of checking whether the grid still belongs to the phase space U of the kinetic system ($F(V) \subset U$) is quite straightforward: all the points $y \in V$ are checked whether they belong to U . If at the next iteration a point $F(y)$ leaves U , then it is pulled inside by a homothety transform with the center in x^* . Since the entropy is a concave function, the homothety contraction with the center in x^* increases the entropy monotonically. Another variant to cut off the points which leave U .

By construction (17), the kernel of the entropic projector is annulled by the entropy differential. Thus, in the first order, the steps in the Newton method with incomplete linearization (31) as well as in the relaxation method (33) do not change the entropy. But if the steps are quite large, then the increase of the entropy may become essential, and the points are returned on their entropy levels by the homothety contraction with the center in the equilibrium point.

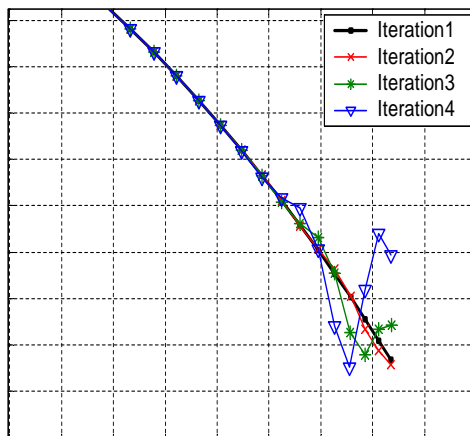


Figure 3: Grid instability. For small grid steps approximations in the calculation of grid derivatives lead to the grid instability effect. Several successive iterations of the algorithm without adaptation of the time step are shown that lead to undesirable “oscillations”, which eventually destroy the grid starting from one of its ends.

5 Instability of fine grids

When one reduces the grid spacing in order to refine the grid, then, once the grid spacing becomes small enough, one can face the problem of the *Courant instability* [17, 18, 19]. Instead of converging, at every iteration the grid becomes more and more entangled (see Fig. 3).

A way to avoid such instability is well-known. This is decreasing the time step. In our problem, instead of a true time step, we have a shift in the Newtonian direction. Formally, we can assign the value $h = 1$ for one complete step in the Newtonian direction. Let us extend now the Newton method to arbitrary h . For this, let us find $\delta x = \delta F(y)$ from (31), but update δx proportionally to h ; the new value of $x_{n+1} = F_{n+1}(y)$ is equal to

$$F_{n+1}(y) = F_n(y) + h_n \delta F_n(y) \quad (35)$$

where n denotes the number of iteration.

One way to choose the step value h is to make it adaptive, by controlling the average value of the invariance defect $\|\Delta_y\|$ at every step. Another way is the convergence control: then $\sum h_n$ plays a role of time.

Elimination of the Courant instability for the relaxation method can be done quite analogously. Everywhere the step h is maintained as large as it is possible without running into convergence problems.

6 Analyticity and effect of superresolution.

When constructing invariant grids, one must define the differential operators (26) for every grid’s node. For calculating the differential operators in some point y , an interpolation procedure in the neighborhood of y is used. As a rule, it is an interpolation by a low-order polynomial, which is constructed using the function values in the nodes belonging to the neighbourhood of y in G . This approximation (using values in the nearest neighborhood nodes) is natural for smooth functions. But we are looking for the *analytical* invariant manifold. Analytical functions have a much more “rigid” structure than the smooth ones. One can change a smooth function in the

neighborhood of any point in such a way, that outside this neighborhood the function will not change. In general, this is not possible for analytical functions: a kind of a “long-range” effect takes place (as is well known) .

The idea is to make use of this effect and to reconstruct some analytical function f_G using a function given on G . There is one important requirement: if the values given on G are values of some function f which is analytical in a neighborhood U , then, if the G is refined “correctly”, one must have $f_G \rightarrow f$ in U . The sequence of reconstructed function f_G should converge to the “right” function f .

What is the “correct refinement”? For smooth functions for the convergence $f_G \rightarrow f$ it is necessary and sufficient that, in the course of refinement, G would approximate the whole U with arbitrary accuracy. For analytical functions it is necessary only that, under the refinement, G would approximate some uniqueness set $A \subset U$. A subset $A \subset U$ is called *uniqueness set* in U if for analytical in U functions ψ and φ from $\psi|_A \equiv \varphi|_A$ it follows $\psi \equiv \varphi$. Suppose we have a sequence of grids G , each next is finer than the previous, which approximate a set A . For smooth functions using function values defined on the grids one can reconstruct the function in A . For analytical functions, if the analyticity domain U is known, and A is a uniqueness set in U , then one can reconstruct the function in U . The set U can be essentially bigger than A ; because of this such extension was named as *superresolution effect* [20]. There exist formulas for construction of analytical functions f_G for different domains U , uniqueness sets $A \subset U$ and for different ways of discrete approximation of A by a sequence of refined grids G [20]. Here we provide only one Carleman’s formula which is the most appropriate for our purposes.

Let domain $U = Q_\sigma^n \subset C^n$ be a product of strips $Q_\sigma \subset C$, $Q_\sigma = \{z | \text{Im} z < \sigma\}$. We shall construct functions holomorphic in Q_σ^n . This is effectively equivalent to the construction of real analytical functions f in the whole R^n with a condition on the convergence radius $r(x)$ of the Taylor series for f as a function of each coordinate: $r(x) \geq \sigma$ in every point $x \in R^n$.

The sequence of refined grids is constructed as follows: let for every $l = 1, \dots, n$ a finite sequence of distinct points $N_l \subset Q_\sigma$ be defined:

$$N_l = \{x_{lj} | j = 1, 2, 3, \dots\}, x_{lj} \neq x_{li} \text{ for } i \neq j \quad (36)$$

The countable uniqueness set A , which is approximated by a sequence of refined grids, has the form:

$$A = N_1 \times N_2 \times \dots \times N_n = \{(x_{1i_1}, x_{2i_2}, \dots, x_{ni_n}) | i_{1, \dots, n} = 1, 2, 3, \dots\} \quad (37)$$

The grid G_m is defined as the product of initial fragments N_l of length m :

$$G_m = \{(x_{1i_1}, x_{2i_2}, \dots, x_{ni_n}) | 1 \leq i_{1, \dots, n} \leq m\} \quad (38)$$

Let us denote $\lambda = 2\sigma/\pi$ (σ is a half-width of the strip Q_σ). The key role in the construction of the Carleman’s formula is played by the functional $\omega_m^\lambda(u, p, l)$ of 3 variables: $u \in U = Q_\sigma^n$, p is an integer, $1 \leq p \leq m$, l is an integer, $1 \leq l \leq n$. Further u will be the coordinate value at the point where the extrapolation is calculated, l will be the coordinate number, and p will be an element of multi-index $\{i_1, \dots, i_n\}$ for the point $(x_{1i_1}, x_{2i_2}, \dots, x_{ni_n}) \in G$:

$$\begin{aligned} \omega_m^\lambda(u, p, l) &= \frac{(e^{\lambda x_{lp}} + e^{\lambda \bar{x}_{lp}})(e^{\lambda u} - e^{\lambda x_{lp}})}{\lambda(e^{\lambda u} + e^{\lambda \bar{x}_{lp}})(u - x_{lp})e^{\lambda x_{lp}}} \\ &\times \prod_{j=1, j \neq p}^m \frac{(e^{\lambda x_{lp}} + e^{\lambda \bar{x}_{lj}})(e^{\lambda u} - e^{\lambda x_{lj}})}{(e^{\lambda x_{lp}} - e^{\lambda x_{lj}})(e^{\lambda u} + e^{\lambda \bar{x}_{lj}})} \end{aligned} \quad (39)$$

For real-valued x_{pk} formula (39) simplifies:

$$\omega_m^\lambda(u, p, l) = 2 \frac{e^{\lambda u} - e^{\lambda x_{lp}}}{\lambda(e^{\lambda u} + e^{\lambda x_{lp}})(u - x_{lp})} \times \prod_{j=1, j \neq p}^m \frac{(e^{\lambda x_{lp}} + e^{\lambda x_{lj}})(e^{\lambda u} - e^{\lambda x_{lj}})}{(e^{\lambda x_{lp}} - e^{\lambda x_{lj}})(e^{\lambda u} + e^{\lambda x_{lj}})} \quad (40)$$

The Carleman formula for extrapolation from G_M on $U = Q_\sigma^n$ ($\sigma = \pi\lambda/2$) has the form ($z = (z_1, \dots, z_n)$):

$$f_m(z) = \sum_{k_1, \dots, k_n=1}^m f(x_k) \prod_{j=1}^n \omega_m^\lambda(z_j, k_j, j), \quad (41)$$

where $k = k_1, \dots, k_n$, $x_k = (x_{1k_1}, x_{2k_2}, \dots, x_{nk_n})$.

There exists a theorem [20]:

If $f \in H^2(Q_\sigma^n)$, then $f(z) = \lim_{m \rightarrow \infty} f_m(z)$, where $H^2(Q_\sigma^n)$ is the Hardy class of holomorphic in Q_σ^n functions.

It is useful to present the asymptotics of (41) for large $|\operatorname{Re} z_j|$. For this purpose, we shall consider the asymptotics of (41) for large $|\operatorname{Re} u|$:

$$|\omega_m^\lambda(u, p, l)| = \left| \frac{2}{\lambda u} \prod_{j=1, j \neq p}^m \frac{e^{\lambda x_{lp}} + e^{\lambda x_{lj}}}{e^{\lambda x_{lp}} - e^{\lambda x_{lj}}} \right| + o(|\operatorname{Re} u|^{-1}). \quad (42)$$

From the formula (41) one can see that for the finite m and $|\operatorname{Re} z_j| \rightarrow \infty$ function $|f_m(z)|$ behaves like $\text{const} \cdot \prod_j |z_j|^{-1}$.

This property (zero asymptotics) must be taken into account when using the formula (41). When constructing invariant manifolds $F(W)$, it is natural to use (41) not for the immersion $F(y)$, but for the deviation of $F(y)$ from some analytical ansatz $F_0(y)$ [21, 22, 23].

The analytical ansatz $F_0(y)$ can be obtained using Taylor series, just as in the Lyapunov auxiliary theorem [24]. Another variant is to use Taylor series for the construction of Pade-approximations.

It is natural to use approximations (41) in terms of dual variables as well, since there exists for them (as the examples demonstrate) a simple and effective linear ansatz for the invariant manifold. This is the slow invariant subspace E_{slow} of the operator of linearized system (1) in dual variables at the equilibrium point. This invariant subspace corresponds to the set of “slow” eigenvalues (with small $|\operatorname{Re} \lambda|$, $\operatorname{Re} \lambda < 0$). In the space of concentrations this invariant subspace is the quasiequilibrium manifold. It consists of the maximum entropy points on the affine manifolds of the form $x + E_{\text{fast}}$, where E_{fast} is the “fast” invariant subspace of the operator of the linearized system (1) at the equilibrium point. It corresponds to the “fast” eigenvalues (large $|\operatorname{Re} \lambda|$, $\operatorname{Re} \lambda < 0$).

Carleman’s formulas can be useful for the invariant grids construction in two places: first, for the definition of the grid differential operators (26), and second, for the analytical continuation of the manifold from the grid.

7 Example: Two-step catalytic reaction

Let us consider a two-step four-component reaction with one catalyst A_2 (the Michaelis-Menten mechanism, see Fig. 1a):



We assume the Lyapunov function of the form

$$S = -G = -\sum_{i=1}^4 c_i [\ln(c_i/c_i^{\text{eq}}) - 1].$$

The kinetic equation for the four-component vector of concentrations, $\mathbf{c} = (c_1, c_2, c_3, c_4)$, has the form

$$\dot{\mathbf{c}} = \gamma_1 W_1 + \gamma_2 W_2. \quad (44)$$

Here $\gamma_{1,2}$ are stoichiometric vectors,

$$\gamma_1 = (-1, -1, 1, 0), \quad \gamma_2 = (0, 1, -1, 1), \quad (45)$$

while functions $W_{1,2}$ are reaction rates:

$$W_1 = k_1^+ c_1 c_2 - k_1^- c_3, \quad W_2 = k_2^+ c_3 - k_2^- c_2 c_4. \quad (46)$$

Here $k_{1,2}^\pm$ are reaction rate constants. The system under consideration has two conservation laws,

$$c_1 + c_3 + c_4 = B_1, \quad c_2 + c_3 = B_2, \quad (47)$$

or $\langle \mathbf{b}_{1,2}, \mathbf{c} \rangle = B_{1,2}$, where $\mathbf{b}_1 = (1, 0, 1, 1)$ and $\mathbf{b}_2 = (0, 1, 1, 0)$. The nonlinear system (43) is effectively two-dimensional, and we consider a one-dimensional reduced description. For our example, we chose the following set of parameters:

$$\begin{aligned} k_1^+ &= 0.3, \quad k_1^- = 0.15, \quad k_2^+ = 0.8, \quad k_2^- = 2.0; \\ c_1^{\text{eq}} &= 0.5, \quad c_2^{\text{eq}} = 0.1, \quad c_3^{\text{eq}} = 0.1, \quad c_4^{\text{eq}} = 0.4; \\ B_1 &= 1.0, \quad B_2 = 0.2 \end{aligned} \quad (48)$$

The one-dimensional invariant grid is shown in Fig. 4 in the (c_1, c_4, c_3) coordinates. The grid was constructed by the growing lump method, as described above. We used Newton iterations to adjust the nodes. The grid was grown up to the boundaries of the phase space.

The grid in this example is a one-dimensional ordered sequence $\{x_1, \dots, x_n\}$. The grid derivatives for calculating the tangent vectors g were taken as $g(x_i) = (x_{i+1} - x_{i-1}) / \|x_{i+1} - x_{i-1}\|$ for the internal nodes, and $g(x_1) = (x_1 - x_2) / \|x_1 - x_2\|$, $g(x_n) = (x_n - x_{n-1}) / \|x_n - x_{n-1}\|$ for the grid's boundaries.

Close to the phase space boundaries we had to apply an adaptive algorithm for choosing the time step h : if, after the next growing step (adding new nodes to the grid and after completing $N = 20$ Newtonian steps, the grid did not converged, then we choose a new step size $h_{n+1} = h_n/2$ and recalculate the grid. The final (minimal) value for h was $h \approx 0.001$.

The location of the nodes was parametrized with the entropic distance to the equilibrium point measured in the quadratic metrics given by the matrix $\mathbf{H}_c = -\|\partial^2 S(\mathbf{c}) / \partial c_i \partial c_j\|$ in the equilibrium c^{eq} . It means that every node is located on a sphere in this metrics with a given radius, which increases linearly with number of the node. In this figure the step of the increase is chosen to be 0.05. Thus, the first node is at the distance 0.05 from the equilibrium, the second is at the distance 0.10 and so on. Fig. 5 shows several important quantities which facilitate understanding of the object (invariant grid) extracted. The sign on the x-axis of the graphs at Fig. 5 is meaningless since the distance is always positive, but in this situation it indicates two possible directions from the equilibrium point.

Fig. 5a,b represents the slow one-dimensional component of the dynamics of the system. Given any initial condition, the system quickly finds the corresponding point on the manifold and starting from this point the dynamics is given by a part of the graph on the Fig. 5a,b.

One of the useful quantities is shown on the Fig. 5c. It is the relation between the relaxation times “toward” and “along” the grid (λ_2/λ_1 , where λ_1, λ_2 are the smallest and the next smallest by absolute value non-zero eigenvalue of the system, symmetrically linearized at the point of the grid node). The figure demonstrates that the system is very stiff close to the equilibrium point (λ_1 and λ_2 are well separated from each other), and becomes less stiff (by order of magnitude) near the boundary. This leads to the conclusion that the one-dimensional reduced model is more adequate in the neighborhood of the equilibrium where fast and slow motions are separated by two orders of magnitude. On the end-points of the grid the one-dimensional reduction ceases to be well-defined.

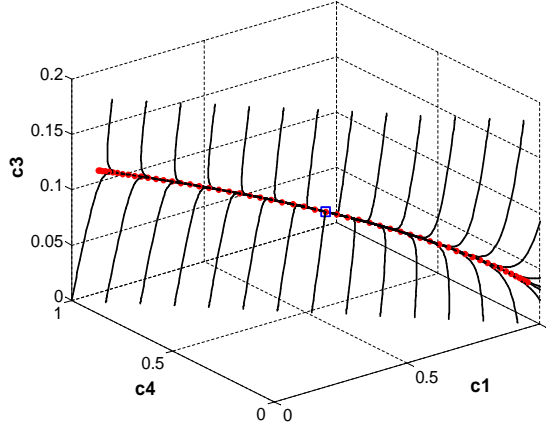
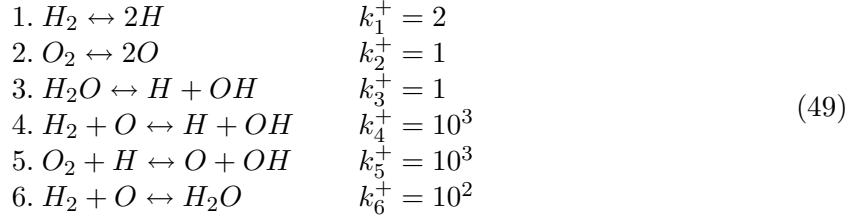


Figure 4: One-dimensional invariant grid (circles) for the two-dimensional chemical system. Projection into the 3d-space of c_1 , c_4 , c_3 concentrations. The trajectories of the system in the phase space are shown by lines. The equilibrium point is marked by the square. The system quickly reaches the grid and further moves along it.

8 Example: Model hydrogen burning reaction

In this section we consider a more complicated example (see Fig. 1b), where the concentration space is 6-dimensional, while the system is 4-dimensional. We construct an invariant flag which consists of 1- and 2-dimensional invariant manifolds.

We consider a chemical system with six species called H_2 (hydrogen), O_2 (oxygen), H_2O (water), H , O , OH (radicals), see Fig. 1. We assume the Lyapunov function of the form $S = -G = -\sum_{i=1}^6 c_i [\ln(c_i/c_i^{\text{eq}}) - 1]$. The subset of the hydrogen burning reaction and corresponding (direct) rate constants have been taken as:



The conservation laws are:

$$\begin{aligned}
 2c_{H_2} + 2c_{H_2O} + c_H + c_{OH} &= b_H \\
 2c_{O_2} + c_{H_2O} + c_O + c_{OH} &= b_O
 \end{aligned} \tag{50}$$

For parameter values we took $b_H = 2$, $b_O = 1$, and the equilibrium point:

$$c_{H_2}^{\text{eq}} = 0.27 \quad c_{O_2}^{\text{eq}} = 0.135 \quad c_{H_2O}^{\text{eq}} = 0.7 \quad c_H^{\text{eq}} = 0.05 \quad c_O^{\text{eq}} = 0.02 \quad c_{OH}^{\text{eq}} = 0.01 \tag{51}$$

Other rate constants k_i^- , $i = 1..6$ were calculated from c^{eq} value and k_i^+ . For this system the stoichiometric vectors are:

$$\begin{aligned}
 \gamma_1 &= (-1, 0, 0, 2, 0, 0) & \gamma_2 &= (0, -1, 0, 0, 2, 0) \\
 \gamma_3 &= (0, 0, -1, 1, 0, 1) & \gamma_4 &= (-1, 0, 0, 1, -1, 1) \\
 \gamma_5 &= (0, -1, 0, -1, 1, 1) & \gamma_6 &= (-1, 0, 1, 0, -1, 0)
 \end{aligned} \tag{52}$$

The system under consideration is fictitious in the sense that the subset of equations corresponds to the simplified picture of this chemical process and the rate constants do not correspond

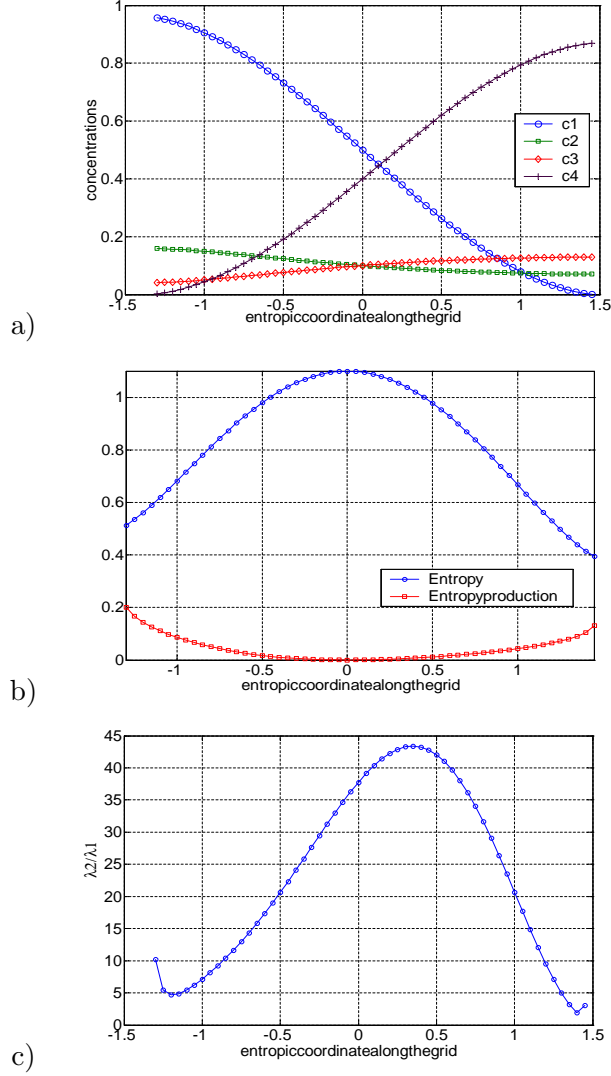


Figure 5: One-dimensional invariant grid for the two-dimensional chemical system. a) Values of the concentrations along the grid. b) Values of the entropy and the entropy production ($-dG/dt$) along the grid. c) Ratio of the relaxation times “towards” and “along” the manifold. The nodes positions are parametrized with entropic distance measured in the quadratic metrics given by $\mathbf{H}_c = -\|\partial^2 S(\mathbf{c})/\partial c_i \partial c_j\|$ in the equilibrium \mathbf{c}^{eq} . Entropic coordinate equal to zero corresponds to the equilibrium.

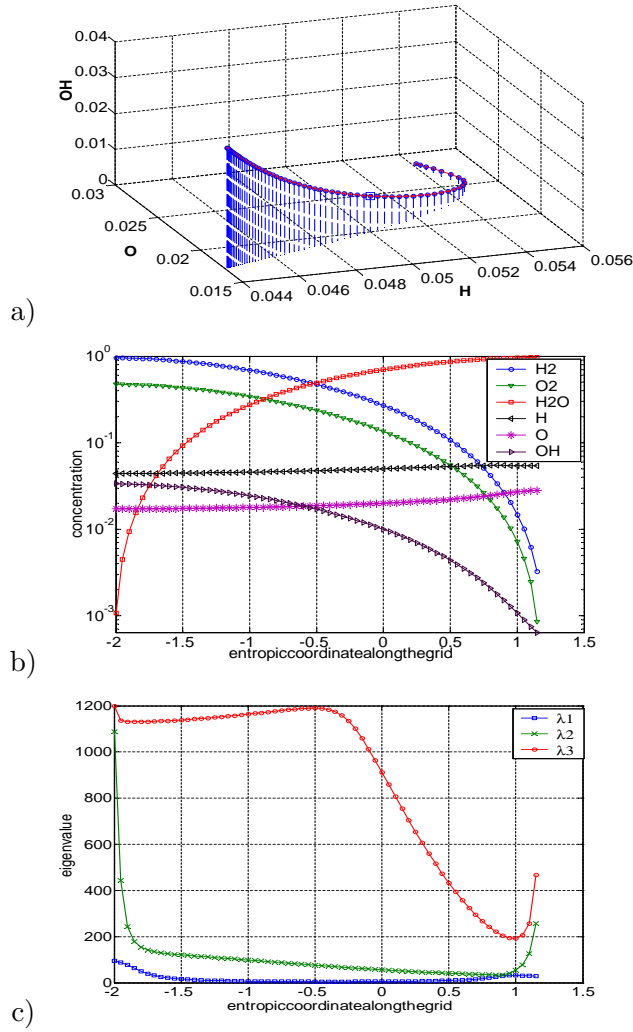


Figure 6: One-dimensional invariant grid for model hydrogen burning reaction. a) Projection into the 3d-space of c_H , c_O , c_{OH} concentrations. b) Concentration values along the grid. c) Three smallest by the absolute value non-zero eigenvalues of the symmetrically linearized system.

to any experimentally measured quantities, rather they reflect only orders of magnitudes relevant real-world systems. In that sense we consider here a qualitative model system, which allows us to illustrate the invariant grids method. Nevertheless, modeling of more realistic systems differs only in the number of species and equations. This leads, of course, to computationally harder problems, but difficulties are not crucial.

Fig. 6a presents a one-dimensional invariant grid constructed for the system. Fig. 6b demonstrates the reduced dynamics along the manifold (for the explanation of the meaning of the x -coordinate, see the previous subsection). In Fig. 6c the three smallest by the absolute value non-zero eigenvalues of the symmetrically linearized Jacobian matrix of the system are shown. One can see that the two smallest eigenvalues almost interchange on one of the grid ends. This means that the one-dimensional “slow” manifold faces definite problems in this region, it is just not well defined there. In practice, it means that one has to use at least a two-dimensional grids there.

Fig. 7a gives a view of the two-dimensional invariant grid, constructed for the system, using the “invariant flag” strategy. The grid was raised starting from the 1D-grid constructed at the previous step. At the first iteration for every node of the initial grid, two nodes (and two

edges) were added. The direction of the step was chosen as the direction of the eigenvector of the matrix A^{sym} (at the point of the node), corresponding to the second “slowest” direction. The value of the step was chosen to be $\epsilon = 0.05$ in terms of entropic distance. After several Newton’s iterations done until convergence was reached, new nodes were added in the direction “ortogonal” to the 1D-grid. This time it was done by linear extrapolation of the grid on the same step $\epsilon = 0.05$. Once some new nodes become one or several negative coordinates (the grid reaches the boundaries) they were cut off. If a new node has only one edge, connecting it to the grid, it was excluded (since it was impossible to calculate 2D-tangent space for this node). The process was continued until the expansion was possible (the ultimate state is when every new node had to be cut off).

The method for calculating tangent vectors for this regular rectangular 2D-grid was chosen to be quite simple. The grid consists of *rows*, which are co-oriented by construction to the initial 1D-grid, and *columns* that consist of the adjacent nodes in the neighboring rows. The direction of the columns corresponds to the second slowest direction along the grid. Then, every row and column is considered as a 1D-grid, and the corresponding tangent vectors are calculated as it was described before:

$$g_{row}(x_{k,i}) = (x_{k,i+1} - x_{k,i-1}) / \|x_{k,i+1} - x_{k,i-1}\|$$

for the internal nodes and

$$\begin{aligned} g_{row}(x_{k,1}) &= (x_{k,1} - x_{k,2}) / \|x_{k,1} - x_{k,2}\|, g_{row}(x_{k,n_k}) \\ &= (x_{k,n_k} - x_{k,n_k-1}) / \|x_{k,n_k} - x_{k,n_k-1}\| \end{aligned}$$

for the nodes which are close to the grid’s edges. Here $x_{k,i}$ denotes the vector of the node in the k th row, i th column; n_k is the number of nodes in the k th row. Second tangent vector $g_{col}(x_{k,i})$ is calculated analogously. In practice, it proves convenient to orthogonalize $g_{row}(x_{k,i})$ and $g_{col}(x_{k,i})$.

9 Invariant grid as a tool for visualization of dynamic system properties

Usual way of dealing with a system (1) is to define some initial conditions and solve the equation for a given time interval. This gives us one particular trajectory of the system. Can we have a look at the global picture of all possible trajectories or in other words can we visualize the vector field in R^N , defined by $\mathbf{J}(x)$? It would be possible if one has two or three species in the system (1). Invariant manifolds and their grid representation allow to do it for higher dimensions, thus they can serve as a data visualization tool. The situation is somewhat close in spirit with data visualization using principal manifolds (for example, see [11]) where one uses two-dimensional manifolds to visualize a finite set of points. Invariant manifolds allow to visualize the global system dynamics on the non-linear manifold of slow motions (i.e., in the space which corresponds to the effects observed in a real-life experiment).

In this section we demonstrate global system dynamics visualization on the model hydrogen burning reaction. Since the phase space is four-dimensional, it is impossible to visualize the grid in one of the coordinate 3D-views, as it was done in the previous subsection. To facilitate visualization one can utilize traditional methods of multi-dimensional data visualization. Here we make use of the principal components analysis (see, for example, [12]), which constructs a three-dimensional linear subspace with maximal dispersion of the orthogonally projected data (grid nodes in our case). In other words, the method of principal components constructs in a multi-dimensional space a three-dimensional box such that the grid can be placed maximally

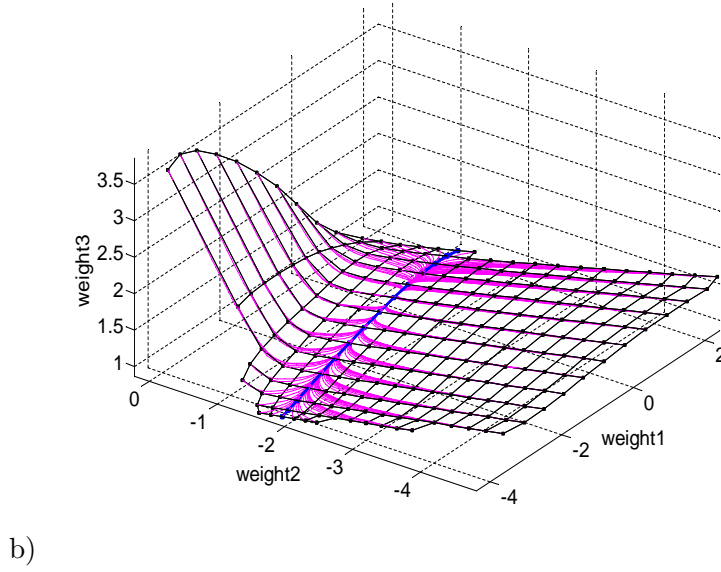
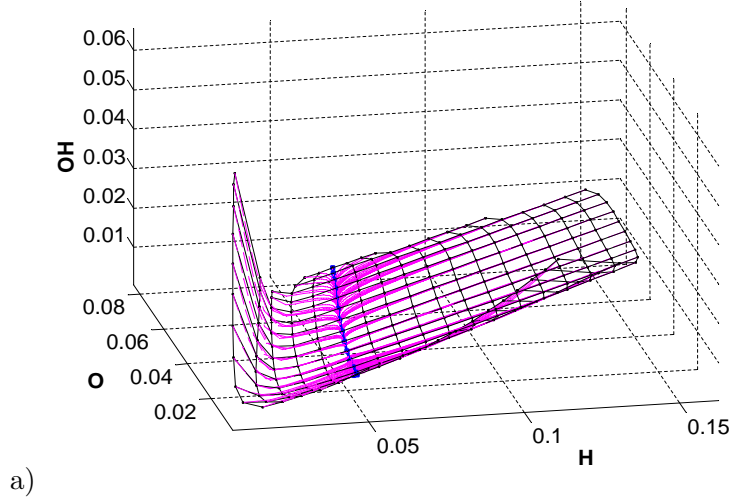


Figure 7: Two-dimensional invariant grid for the model hydrogen burning reaction. a) Projection into the 3d-space of c_H , c_O , c_{OH} concentrations. b) Projection into the principal 3D-subspace. Trajectories of the system are shown coming out from every node. Bold line denotes the one-dimensional invariant grid, starting from which the 2D-grid was constructed.

tightly inside the box (in the mean square distance meaning). After projection of the grid nodes into this space, we get more or less adequate representation of the two-dimensional grid embedded into the six-dimensional concentrations space (Fig. 7b). The disadvantage of the approach is that the axes now do not bear any explicit physical meaning, they are just some linear combinations of the concentrations.

One attractive feature of two-dimensional grids is the possibility to use them as a screen, on which one can display different functions $f(\mathbf{c})$ defined in the concentrations space. This technology was exploited widely in the non-linear data analysis by the elastic maps method [10], [11]. The idea is to “unfold” the grid on a plane (to present it in the two-dimensional space, where the nodes form a regular lattice). In other words, we are going to work in the internal coordinates of the grid. In our case, the first internal coordinate (let’s call it s_1) corresponds to the direction, co-oriented with the one-dimensional invariant grid, the second one (let us call it s_2) corresponds to the second slow direction. By the construction, the coordinate line $s_2 = 0$ line corresponds to the one-dimensional invariant grid. Units of s_1 and s_2 is the entropic distance.

Every grid node has two internal coordinates (s_1, s_2) and, simultaneously, corresponds to a vector in the concentration space. This allows us to map any function $f(\mathbf{c})$ from the multi-dimensional concentration space to the two-dimensional space of the grid. This mapping is defined in a finite number of points (grid nodes), and can be interpolated (linearly, in the simplest case) between them. Using *coloring* and *isolines* one can visualize the values of the function in the neighborhood of the invariant manifold. This is meaningful, since, by the definition, the system spends most of the time in the vicinity of the invariant manifold, thus, one can visualize the behavior of the system. As a result of applying this technology, one obtains a set of color illustrations (a stack of information layers), put onto the grid as a map. This enables applying the whole family of the well developed methods of working with the stack of information layers, such as the *geographical information systems* (GIS) methods.

Briefly, this technique of the visualization is a useful tool for understanding of dynamical systems. It allows to see simultaneously many different scenarios of the system behavior, together with different system’s characteristics.

Let us use the invariant grids for the the model hydrogen burning system as a screen for visualisation. The simplest functions to visualize are the coordinates: $c_i(\mathbf{c}) = c_i$. In Fig. 8 we displayed four colorings, corresponding to the four arbitrarily chosen concentrations functions (of H_2 , O , H and OH ; Fig. 8a-d). The qualitative conclusion that can be made from the graphs is that, for example, the concentration of H_2 practically does not change during the first fast motion (towards the 1D-grid) and then, gradually changes to the equilibrium value (the H_2 coordinate is “slow”). The O coordinate is the opposite case, it is the “fast” coordinate which changes quickly (on the first stage of the motion) to the almost equilibrium value, and it almost does not change after that. Basically, the slopes of the coordinate isolines give some impression of how “slow” a given concentration is. Fig. 8c shows an interesting behavior of the OH concentration. Close to the 1D grid it behaves like a “slow coordinate”, but there is a region on the map where it has a clear “fast” behavior (middle bottom of the graph).

The next two functions which one could wish to visualize are the entropy S and the entropy production $\sigma(\mathbf{c}) = -dG/dt(\mathbf{c}) = \sum_i \ln(c_i/c_i^{\text{eq}})\dot{c}_i$. They are shown on Fig. 9a,b.

Finally, we visualize the relation between the relaxation times of the fast motion towards the 2D-grid and the slow motion along it. This is given on the Fig. 9c. This picture allows to make a conclusion that two-dimensional consideration can be appropriate for the system (especially in the “high H_2 , high O ” region), since the relaxation times “towards” and “along” the grid are well separated. One can compare this to the Fig. 9d, where the relation between relaxation times towards and along the 1D-grid is shown.

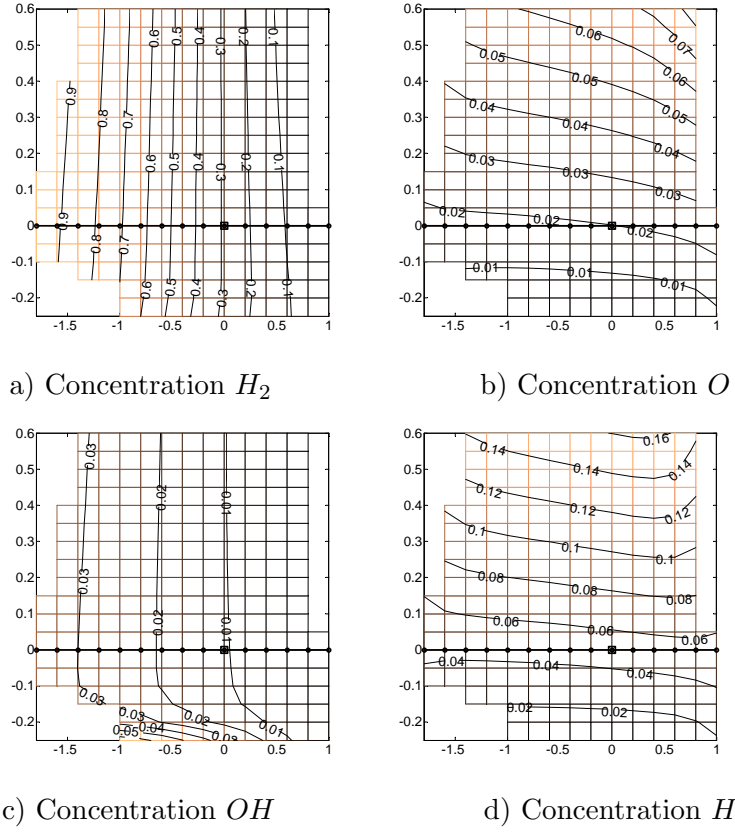


Figure 8: Two-dimensional invariant grid as a screen for visualizing different functions defined in the concentrations space. The coordinate axes are entropic distances (see the text for the explanations) along the first and the second slowest directions on the grid. The corresponding 1D invariant grid is denoted by bold line, the equilibrium is denoted by square.

10 Invariant manifolds for open systems

10.1 Zero-order approximation

Let the initial dissipative system (1) be “spoiled” by an additional term (“external vector field” $J_{ex}(x, t)$):

$$\frac{dx}{dt} = J(x) + J_{ex}(x, t), x \in U. \quad (53)$$

For this new system the entropy does not increase everywhere. In the new system (53) different dynamic effects are possible, such as a non-uniqueness of stationary states, auto-oscillations, etc. The “inertial manifold” effect is well-known: solutions of (53) approach some relatively low-dimensional manifold on which all the non-trivial dynamics takes place [27, 25, 26].

It is natural to expect that the inertial manifold of the system (53) is located somewhere close to the slow manifold of the initial dissipative system (1). This hypothesis has the following basis. Suppose that the vector field $J_{ex}(x, t)$ is sufficiently small. Let’s introduce, for example, a small parameter $\varepsilon > 0$, and consider $\varepsilon J_{ex}(x, t)$ instead of $J_{ex}(x, t)$. Let’s assume that for the system (1) a separation of motions into “slow” and “fast” takes place. In this case, there exists such interval of positive ε that $\varepsilon J_{ex}(x, t)$ is comparable to J only in a small neighborhood of the given slow motion manifold of the system (1). Outside this neighborhood, $\varepsilon J_{ex}(x, t)$ is negligibly small in comparison with J and only negligibly influences the motion (for this statement to be

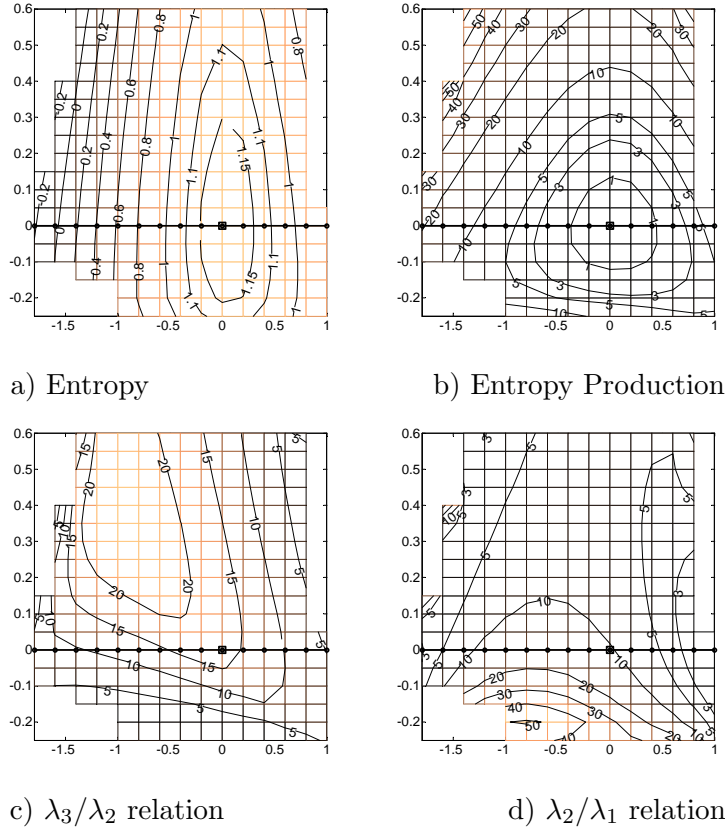


Figure 9: Two-dimensional invariant grid as a screen for visualizing different functions defined in the concentrations space. The coordinate axes are entropic distances (see the text for the explanations) along the first and the second slowest directions on the grid. The corresponding 1D invariant grid is denoted by bold line, the equilibrium is denoted by square.

true, it is important that the system (1) is dissipative and every solution comes in finite time to a small neighborhood of the given slow manifold).

Precisely this perspective on the system (53) allows to exploit slow invariant manifolds constructed for the dissipative system (1) as the ansatz and the zero-order approximation in a construction of the inertial manifold of the open system (53). In the zero-order approximation, the right part of the equation (53) is simply projected onto the tangent space of the slow manifold.

The choice of the projector is determined by the motion separation which was described above: fast motion is taken from the dissipative system (1). A projector which is suitable for all dissipative systems with given entropy function is unique. It is constructed in the following way. Let a point $x \in U$ be defined and some vector space T , on which one needs to construct a projection (T is the tangent space to the slow manifold at the point x). We introduce the entropic scalar product $\langle | \rangle_x$:

$$\langle a | b \rangle_x = -(a, D_x^2 S(b)). \quad (54)$$

Let us consider T_0 that is a subspace of T and which is annulled by the differential S at the point x .

$$T_0 = \{a \in T | D_x S(a) = 0\} \quad (55)$$

If $T_0 = T$, then the thermodynamic projector is the orthogonal projector on T with respect

to the entropic scalar product $\langle | \rangle_x$. Suppose that $T_0 \neq T$. Let $e_g \in T$, $e_g \perp T_0$ with respect to the entropic scalar product $\langle | \rangle_x$, and $D_x S(e_g) = 1$. These conditions define vector e_g uniquely.

The projector onto T is defined by the formula

$$P(J) = P_0(J) + e_g D_x S(J) \quad (56)$$

where P_0 is the orthogonal projector onto T_0 with respect to the entropic scalar product $\langle | \rangle_x$. For example, if T a finite-dimensional space, then the projector (56) is constructed in the following way. Let e_1, \dots, e_n be a basis in T , and for definiteness, $D_x S(e_1) \neq 0$.

1) Let us construct a system of vectors

$$b_i = e_{i+1} - \lambda_i e_1, (i = 1, \dots, n-1), \quad (57)$$

where $\lambda_i = D_x S(e_{i+1})/D_x S(e_1)$, and hence $D_x S(b_i) = 0$. Thus, $\{b_i\}_1^{n-1}$ is a basis in T_0 .

2) Let us orthogonalize $\{b_i\}_1^{n-1}$ with respect to the entropic scalar product $\langle | \rangle_x$ (1). We thus derived an orthonormal with respect to $\langle | \rangle_x$ basis $\{g_i\}_1^{n-1}$ in T_0 .

3) We find $e_g \in T$ from the conditions:

$$\langle e_g | g_i \rangle_x = 0, (i = 1, \dots, n-1), D_x S(e_g) = 1. \quad (58)$$

and, finally we get

$$P(J) = \sum_{i=1}^{n-1} g_i \langle g_i | J \rangle_x + e_g D_x S(J). \quad (59)$$

If $D_x S(T) = 0$, then the projector P is simply the orthogonal projector with respect to the $\langle | \rangle_x$ scalar product. This is possible if x is the global maximum of entropy point (equilibrium). Then

$$P(J) = \sum_{i=1}^n g_i \langle g_i | J \rangle_x, \langle g_i | g_j \rangle = \delta_{ij}. \quad (60)$$

10.2 First-order approximation

Thermodynamic projector (56) defines a "slow and fast motions" duality: if T is the tangent space of the slow motion manifold then $T = \text{im} P$, and $\ker P$ is the plane of fast motions. Let us denote by P_x the projector at a point x of a given slow manifold.

The vector field $J_{ex}(x, t)$ can be decomposed in two components:

$$J_{ex}(x, t) = P_x J_{ex}(x, t) + (1 - P_x) J_{ex}(x, t). \quad (61)$$

Let us denote $J_{exs} = P_x J_{ex}$, $J_{exf} = (1 - P_x) J_{ex}$. The slow component J_{exs} gives a correction to the motion along the slow manifold. This is a zero-order approximation. The "fast" component shifts the slow manifold in the fast motions plane. This shift changes $P_x J_{ex}$ accordingly. Consideration of this effect gives a first-order approximation. In order to find it, let us rewrite the invariance equation taking J_{ex} into account:

$$\begin{cases} (1 - P_x)(J(x + \delta x) + \varepsilon J_{ex}(x, t)) = 0 \\ P_x \delta x = 0 \end{cases} \quad (62)$$

The first iteration of the Newton method subject to incomplete linearization gives:

$$\begin{cases} (1 - P_x)(D_x J(\delta x) + \varepsilon J_{ex}(x, t)) = 0 \\ P_x \delta x = 0. \end{cases} \quad (63)$$

$$(1 - P_x)D_x J(1 - P_x)J(\delta x) = -\varepsilon J_{ex}(x, t). \quad (64)$$

Thus, we have derived a linear equation in the space $\ker P$. The operator $(1 - P)D_x J(1 - P)$ is defined in this space.

Utilization of the self-adjoint linearization instead of the traditional linearization $D_x J$ operator considerably simplifies solving and studying equation (64). It is necessary to take into account here that the projector P is a sum of the orthogonal projector with respect to the $\langle | \rangle_x$ scalar product and a projector of rank one.

Assume that the first-order approximation equation (64) has been solved and the following function has been found:

$$\delta_1 x(x, \varepsilon J_{ex} f) = -[(1 - P_x)D_x J(1 - P_x)]^{-1} \varepsilon J_{ex} f, \quad (65)$$

where $D_x J$ is either the differential of J or symmetrized differential of J (20).

Let x be a point on the initial slow manifold. At the point $x + \delta x(x, \varepsilon J_{ex} f)$ the right-hand side of equation (53) in the first-order approximation is given by

$$J(x) + \varepsilon J_{ex}(x, t) + D_x J(\delta x(x, \varepsilon J_{ex} f)). \quad (66)$$

Due to the first-order approximation (66), the motion of a point projection onto the manifold is given by the following equation

$$\frac{dx}{dt} = P_x(J(x) + \varepsilon J_{ex}(x, t) + D_x J(\delta x(x, \varepsilon J_{ex} f(x, t)))). \quad (67)$$

Note that, in equation (67), the vector field $J(x)$ enters only in the form of projection, $P_x J(x)$. For the invariant slow manifold it holds $P_x J(x) = J(x)$, but actually we always deal with approximately invariant manifolds, hence, it is necessarily to use the projection $P_x J$ instead of J in (67).

Remark. The notion "projection of a point onto the manifold" needs to be specified. For every point x of the slow invariant manifold M there are defined both the thermodynamic projector P_x (56) and the fast motions plane $\ker P_x$. Let us define a projector Π of some neighborhood of M onto M in the following way:

$$\Pi(z) = x, \text{ if } P_x(z - x) = 0. \quad (68)$$

Qualitatively, it means that z , after all fast motions took place, comes into a small neighborhood of x . The operation (56) is defined uniquely in some small neighborhood of the manifold M .

A derivation of slow motions equations requires not only an assumption that εJ_{ex} is small but it must be slow as well: $\frac{d}{dt}(\varepsilon J_{ex})$ must be small too.

One can get the further approximations for slow motions of the system (53), taking into account the time derivatives of J_{ex} . This is an alternative to the usage of the projection operators methods [28].

11 Conclusion

In this paper we presented a method for reducing complexity in complex chemical reaction networks using a consistent approach of constructing invariant manifold for the system of kinetic equations. The method is applicable to the class of dissipative systems (with Lyapounov function) and can be extended to the case of open systems as well.

An attractive feature of the approach is its clear geometrical interpretation. The geometrical approach becomes more and more popular in applied model reduction: one constructs a slow approximate invariant manifold, and dynamical equations on this manifold instead of an approximation of solutions to the initial equations. After that, the equations on the slow manifold can be studied separately, as well as the fast motion to this manifold (the initial layer problem [29]).

The notion of invariant grid may be useful beyond the chemical kinetics. This discrete invariant object can serve as a representation of approximate slow invariant manifold, and as a screen (a map) for visualization of different functions and properties. The problem of the grid correction is fully decomposed into the problems of the grid's nodes correction which makes it open to effective parallel implementations.

The next step should be the implementation of the method of invariant grids for investigation of high-dimensional systems "kinetics+transport". The asymptotic analysis of the methods of analytic continuation the manifold from the grid should lead to further development of these methods and modifications of the Carleman formula.

12 Acknowledgements

The project is partially supported by Swiss National Science Foundation, Project 200021-107885/1 "Invariant manifolds for model reduction in chemical kinetics" and Swiss Federal Department of Energy (BFE) under the project 100862 "Lattice Boltzmann simulations for chemically reactive systems in a micrometer domain".

References

- [1] Hasty J, McMillen D, Isaacs F, Collins J: Computational studies of gene regulatory networks: in numero molecular biology. *Nat Rev Genet* 2001; 4: 268–79.
- [2] Endy D, Brent R: Modelling cellular behaviour. *Nature* 2001; 409(6818): 391–5.
- [3] Gorban AN, Karlin IV: Thermodynamic parameterization. *Physica A* 1992; 190: 393–404.
- [4] Gorban AN, Karlin IV, Zinovyev AY: Constructive methods of invariant manifolds for kinetic problems. *Phys. Reports* 2004; **396**, 4-6: 197–403. Preprint online: <http://arxiv.org/abs/cond-mat/0311017>.
- [5] Gorban AN, Karlin IV: Method of invariant manifold for chemical kinetics. *Chem. Eng. Sci.* 2003; **58**, 21: 4751–4768. Preprint online: <http://arxiv.org/abs/cond-mat/0207231>.
- [6] Gorban AN, Karlin IV: Invariant Manifolds for Physical and Chemical Kinetics. *Series: Lecture Notes in Physics*, Vol.660. Springer, 2005
- [7] Gorban AN, Karlin IV: Methods of nonlinear kinetics. In Encyclopedia of Life Support Systems, Encyclopedia of Mathematical Sciences. EOLSS Publishers, Oxford, 2004. Preprint online: <http://arXiv.org/abs/cond-mat/0306062>.
- [8] Gorban AN, Karlin IV, Zinovyev AY: Invariant grids for reaction kinetics. *Physica A* 2004; **333**: 106–154. Preprint online: <http://www.ihes.fr/PREPRINTS/P03/Resu/resu-P03-42.html>.
- [9] Gorban AN: Equilibrium encircling. Equations of chemical kinetics and their thermodynamic analysis. Nauka, Novosibirsk, 1984.

- [10] Gorban AN, Zinovyev AYu: Visualization of data by method of elastic maps and its applications in genomics, economics and sociology. Preprint of Institut des Hautes Etudes Scientifiques, 2001. Online: <http://www.ihes.fr/PREPRINTS/M01/Resu/resu-M01-36.html>.
- [11] Gorban AN, Zinovyev AYu: Elastic principal graphs and manifolds. *Computing* 2005. In press.
- [12] Jolliffe IT: Principal component analysis. Springer-Verlag, 1986.
- [13] Gorban AN, Karlin IV: Uniqueness of thermodynamic projector and kinetic basis of molecular individualism. *Physica A* 2004; **336** 3-4: 391–432. Preprint online: <http://arxiv.org/abs/cond-mat/0309638>.
- [14] Gorban AN, Gorban PA, Karlin IV: Legendre integrators, post-processing and quasiequilibrium. *J. Non-Newtonian Fluid Mech.* 2004; **120**: 149–167. Preprint on-line: <http://arxiv.org/pdf/cond-mat/0308488>.
- [15] Ilg P, Karlin IV, Öttinger HC: Canonical distribution functions in polymer dynamics: I. Dilute solutions of flexible polymers. *Physica A* 2002; **315**: 367–385.
- [16] Ilg P, Karlin IV, Kröger M, Öttinger HC: Canonical distribution functions in polymer dynamics: II Liquid-crystalline polymers. *Physica A* 2003; **319**: 134–150.
- [17] Courant R, Friedrichs KO, Lewy H: On the partial difference equations of mathematical physics. *IBM Journal* (March 1967): 215–234.
- [18] Ames WF: Numerical Methods for Partial Differential Equations, 2nd ed. New York, Academic Press, 1977.
- [19] Richtmyer RD, Morton KW: Difference methods for initial value problems, 2nd ed. Wiley-Interscience, New York, 1967.
- [20] Aizenberg L: Carleman’s formulas in complex analysis: Theory and applications. Mathematics and its applications, Vol. 244. Kluwer, 1993.
- [21] Gorban AN, Rossiev AA: Neural network iterative method of principal curves for data with gaps. *Journal of Computer and System Sciences International* 1999; **38**, 5: 825–831.
- [22] Dergachev VA, Gorban AN, Rossiev AA, Karimova LM, Kuandykov EB, Makarenko NG, Steier P: The filling of gaps in geophysical time series by artificial neural networks. *Radio-carbon* 2001; **43**, 2A: 365 – 371.
- [23] Gorban AN, Rossiev A, Makarenko N, Kuandykov Y, Dergachev V: Recovering data gaps through neural network methods. *International Journal of Geomagnetism and Aeronomy* 2002; **3**, 2: 191–197.
- [24] Lyapunov AM: The general problem of the stability of motion. London, Taylor & Francis, 1992.
- [25] Temam R: Infinite-dimensional dynamical systems in mechanics and physics, ed. 2. Applied Math. Sci., Vol 68. New York, Springer Verlag, 1997.
- [26] Constantin P, Foias C, Nicolaenko B, Temam R: Integral manifolds and inertial manifolds for dissipative partial differential equations. Applied Math. Sci., Vol. 70. New York, Springer Verlag, 1988.

- [27] Foias C, Sell GR, Temam R: Inertial manifolds for dissipative nonlinear evolution equations. *Journal of Differential Equations* 1988; **73**: 309–353.
- [28] Grabert H: Projection operator techniques in nonequilibrium statistical mechanics. Berlin, Springer Verlag, 1982.
- [29] Gorban AN, Karlin IV, Zmievskii VB, Nonnenmacher TF: Relaxational trajectories: global approximations. *Physica A* 1996; **231** : 648-672.